

An Image classification with Smart Customised Deep Convolutional Neural Network based Islanding Detection for PV Inverter-Interfaced Grid System

Santhosh Kumar K¹, *Research Scholar, Osmania University, Hyderabad, Telangana*

Dr. P Mallikarjuna Sharma² *Retired Professor, Vasavi college of Engineering, Hyderabad, Telangana*

Dr. M Manjula³, *Professor, Department of Electrical Engineering, Osmania University, Hyderabad, TG*

ABSTRACT An islanding event is a more serious concern for electrical utilities, which occurs when the utility is separated from the rest of the distributed system, mainly in the presence of renewable sources, and is integrated with an electrical system. In this study, we propose a new islanding detection technique based on a deep learning model using a convolutional neural network (CNN). The proposed method is based on time frequency wavelet analysis, which is used to represent the scalogram image (RGB image) obtained from the time series data at the point of common coupling in the proposed system. The time-series data were converted to scalograms, and the CNN was designed to detect islanding and non-islanding events. The efficiency of the proposed model was optimized by creating Deep Learning experiments with three trials of three different hyperparameter tuning and results with higher accuracy and a minimal loss function were obtained.

INDEX TERMS Red Green Blue (RGB) image, scalogram, convolutional neural network (CNN), distributed generation (DG), Islanding Detection, Time-frequency Wavelet Analysis.

Date of Submission: 01-06-2024

Date of Acceptance: 11-07-2024

I. INTRODUCTION

The requirement for stable and improved power quality (PQ), capital investment, liberalization of the energy market, and environmental concerns have contributed to the increased focus on the prompt integration of distributed generation (DG). In a classical electrical power system (EPS), electricity generation is centralized and distributed to customers through transmission and distribution networks. In addition to the benefits and advantages of DG integration, there are new difficulties and flaws in the power system, such as accidental islanding caused by tripping the main utility circuit breaker (CB). Personnel safety, overvoltage, out-of-phase reconnection, PQ, and equipment protection are the key concerns associated with inadvertent islanding [1], [2]. A range of international and local standards provides the criteria and requirements for islanding detection [3]. International guidelines state that islanding should be detected in the range of 0.16 to 2 seconds [4][5]. Therefore, to address this major issue with DG power systems, have focused a lot of attention on the unintended islanding detection problem over the past ten years. The security of a DG power system depends on accurate, dependable, and quick islanding detection technology (IDT).

Currently, more research is being conducted, and various IDT are categorized into three main groups: local, remote, and intelligent approaches. There are three types of local strategies for islanding detection: hybrid, passive and active.

A large non-detection zone (NDZ) and low speed are associated with passive islanding schemes such as under/over voltage and frequency, voltage phase jump, harmonic measurement, etc., while active methods such as slip-mode frequency shift (SMFS), slip-mode voltage shift (SVS), and Sandia frequency shift (SFS) have problems with noise and power quality [6] [7][8]. Conversely, passive islanding techniques with low speed and a wide non-detection zone (NDZ) include voltage phase jump, harmonic measurement, and under/over voltage and frequency [9][10] and [11]. Hybrid schemes combine active and passive techniques, and their implementation is complex [12], [13]. Owing to their complexity and high cost, remote approaches are not practical for small-scale or microgrid systems. They require a contact link and are consistent with large systems.

Compared with local and remote schemes, intelligent islanding detection techniques are considered to be the most reliable and rapid. Fast detection, low NDZ, high precision, and minimal impact on the PQ of the DG power system are the primary causes of this dominance. A hybrid IDT for multiple inverter-based DG that combines Decision Trees and Sandia Frequency Shift. A novel approach based on active and reactive power was presented and to develop DT logic for the classification of islanding and non-islanding events, which quickly corresponds to the NDZ. The IDT was introduced for an inverter-based DG. Rotational invariance was used for

feature extraction at the point of common coupling (PCC) to approximate the signal parameter and naive-Bayes classifier was used for event classification.

An ANN-based global islanding detection solution for several DGs was proposed. An innovative IDT for single-phase inverter-based DG was introduced using an SVM. Based on the SVM classifier, the IDT for a hybrid DG with IEEE 30-bus was proposed. The authors of presented a novel hybrid strategy for NDZ elimination using FL and SFS. The author proposed an islanding detection technique that limits interfering injection using fuzzy positive feedback (PF). An IDT based on ANFIS for inverter-based DG was presented. In a novel ANFIS system methodology for low-voltage inverter-interfaced microgrid islanding detection was proposed.

In this study, a novel IDM based on image categorization using a convolutional neural network (CNN)-based classifier is proposed. With the help of the proposed method, time-series data are transformed into images that convey system information in the form of distinct patterns for both grid-connected and islanded systems. The treatment of the islanding classification problem as an image classification problem is novel in this method. Additionally, by applying picture classification algorithms, we can take advantage of advances in computer vision and image processing technology. These developments were made using both hardware and software. There have been no prior reports on this strategy in the literature. This is an initial attempt to categorize islanding incidents using a CNN and image classification technique.

The rest of this paper is organised in the following manner. Section 2 describes the process of converting time-series data into images. Section 3 gives an account of the system description and the data set that is generated for training and validating the proposed method. Section 4 explains the details about CNNs and their general architecture and also presents design aspects of the CNN that is designed to classify islanding and non-islanding events.

II. THEORITICAL DETAILS

A. SCALOGRAM

The process of converting time-series data to images is presented. The Continuous Wavelet transform of a signal $x(t)$ is defined as any sinusoid as a Scaled(“mother”) reference sine wave $\psi_o = e^{j2\pi F}$

$$X(\tau, s) = \int_{-\infty}^{\infty} x(t) \frac{1}{\sqrt{s}} \psi^* \left(\frac{t-\tau}{s} \right) dt \quad (1)$$

ψ – analytic function

τ - translation parameter

s - scaling parameter

In wavelet analysis, the time–frequency energy density representation obtained by the wavelet transform is called a scalogram. It is defined as the square of the amplitude of the wavelet transform [35]. In simple terms, a scalogram can be defined as a visual representation of wavelet transform, in which x and y axes represent time and frequency, whereas z -axis represents magnitude displayed in terms of the colour gradient in figure 1

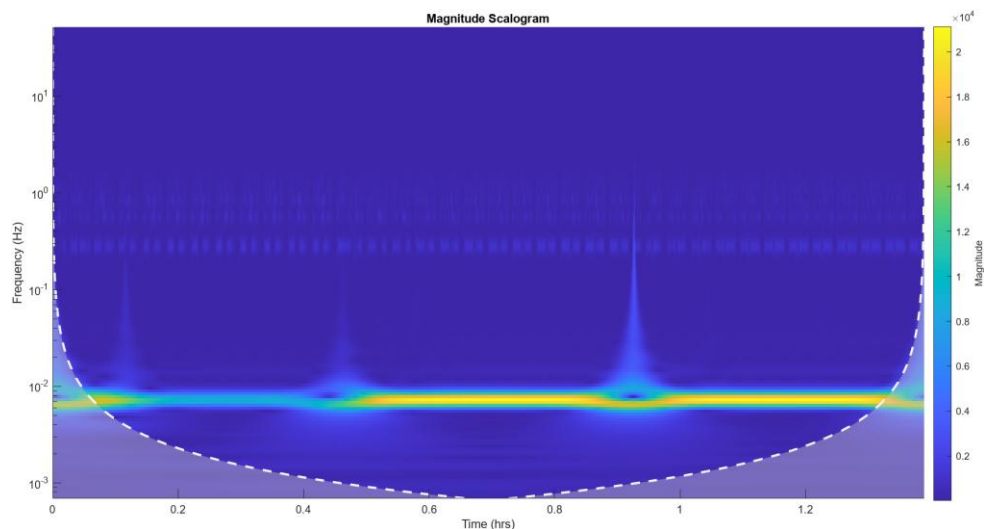


FIGURE 1 Typical Scalogram

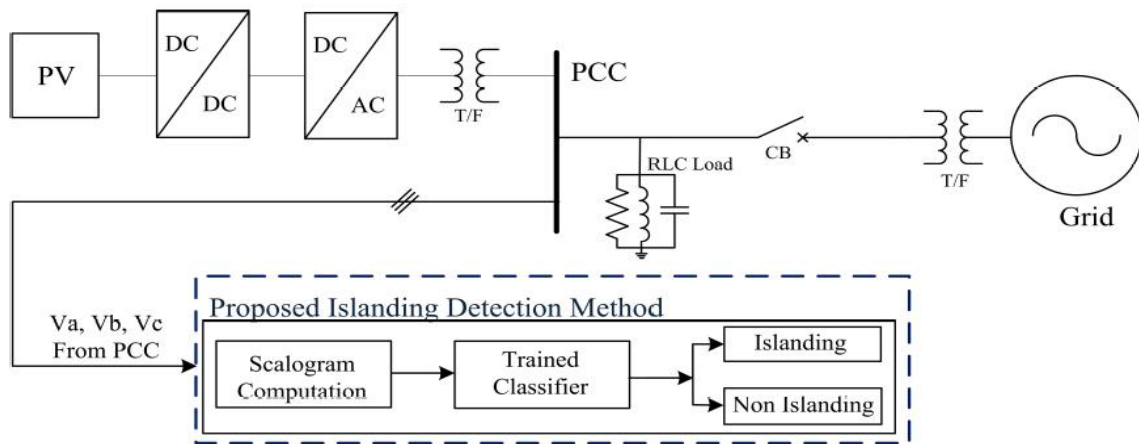


FIGURE 2 Schematic Diagram of Test System

B. GENERATION OF DATASET

Any supervised learning-based method requires a large amount of suitably labelled data to be tested and trained. Standard data sets like ImageNet [14] and MNIST [15] are accessible for picture classification tasks. However, there isn't a common data set like that for islanding detection. Therefore, in order to build a data set, a standard system is needed. Consideration is given to a 2MW grid-connected photovoltaic system to produce the picture data set needed for the suggested method. This system's MATLAB/Simulink model is derived. The model has been modified to align with the specifications of the suggested project. In the MATLAB/Simulink simulations, V_a , V_b , and V_c from the point of common coupling (PCC) are acquired for a total of 6 cycles at 120 samples/second. An islanding event is generated at a time instant of 0.2 s with respect to fault. The simulations are performed using a single CPU running Windows 11 with an Intel Core i5 processor and 16 GB of RAM.

The following procedure is used to create the picture data set for islanding and non-islanding scenarios. A number of islanding and non-islanding events are generated, and for each event, from figure 1, 2 time-series data pertaining to the three-phase voltages V_a , V_b , and V_c from the PCC is obtained. Concatenation is the process of joining two arrays to create a single array. In the case of three-phase voltages, this results in $V[abc]$, which represents the state of each of the three phases together. The concatenated voltage $V[abc]$ is now subjected to CWT in order to produce a scalogram image that contains data from all three phases. After that, these pictures are suitably labelled as either an islanding or non-islanding scenario. The scalogram images of concatenated voltages $V[abc]$ for grid-connected and islanded modes of operation are shown in (see Fig. 3). It is evident from these images that there is a clear distinction between islanded and non-islanded modes of operations, indicating the potential of image classification techniques for islanding detection.

When the power disparity between the DG source generation and the demand is close to nil or minimal, it might be exceedingly challenging to detect an islanding event in the case of most passive IDMs. Several instances with almost no power mismatch are taken into consideration in the data set in order to account for this factor and from figure 3, dataset has generated by varying P and Q values of load.

TABLE 1 Dataset Details

Total Observations	$[V_{abc}]$	1107
Islanding Cases	$[V_{iabc}]$	548
Non-Islanding Cases	$[V_{gabc}]$	559

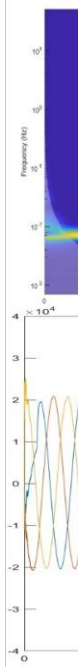


FIGURE 3 Voltage Signal to Scalogram

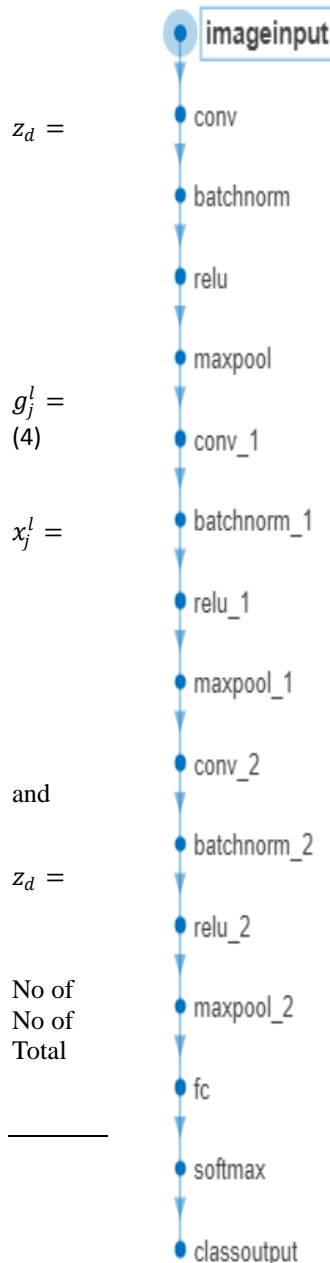


FIGURE4 CNN Architecture

C. Problem formulation

$$\min J(w) = \min_w J(w) = - \sum_d \log Z_d(2)$$

$$\frac{e^{od}}{\sum_{c=1}^C e^{oc}} \rightarrow \frac{e^{x_d^{L-1}}}{\sum_{c=1}^C e^{x_c^{L-1}}} \quad (3)$$

Minimizing the loss function is the objective function with respect to parameters weights and bias.

III. PROPOSED ISLANDING DETECTION TECHNIQUE

A. CNN DESIGN

- Convolution layer

$$x_j^{l-1}(s, t) \times w_{ij}^l = \sum_{\sigma=-n1}^{n1} \sum_{\nu=-n2}^{n2} x_j^{l-i}(s - \sigma, t - \nu) w_{ij}^l(\sigma, \nu)$$

- Activation or ReLu (Rectified linear unit) layer (it introduces non linearity)

$$\max(0, \sum_{i \in M_j} g_j^l + b_j^l) \quad (5)$$

- Max pooling (MP) layer (it picks max values from sub matrix, it performs down sampling of the features that are extracted in the convolution layer, i.e. feature maps)

$$x_j^{l+1} = f_p(b_j^{l+1}(x_j^l) + b_j^{l+1}) \quad (6)$$

- Fully Connected layer (FC)(fully developed model)

$$x^{L-1} = f_c(\beta^{L-1} x^{L-2} + b^{L-1}) \quad (7)$$

- SoftMax layer (n-dimensional vector of real numbers converts them into probabilities for each class and finalizes the loss function)

$$\frac{e^{od}}{\sum_{c=1}^C e^{oc}} \rightarrow \frac{e^{x_d^{L-1}}}{\sum_{c=1}^C e^{x_c^{L-1}}} \quad (8)$$

layers 16
connections 15
learnable parameters 3.3 million

IV. STOCHASTIC GRADIENT DESCENT WITH MOMENTUM ALGORITHM

Stochastic Gradient Descent with Momentum (SGDM) Algorithm

- Step 1: Initialize the model's weights randomly and bias Weight w randomly
- Step 2: Shuffle the training dataset.
- Step 3: compute the gradient of the loss function with respect to the model's weights.
- Step 4: Update the weights using the computed gradient and the learning rate.

$$w_{new} = w_{old} - \alpha \nabla J(w_{old}) \quad (9)$$

- Repeat steps 3–4 until the stopping criterion is met. (Converges- minimum point with respect to minimum weight of the loss function)

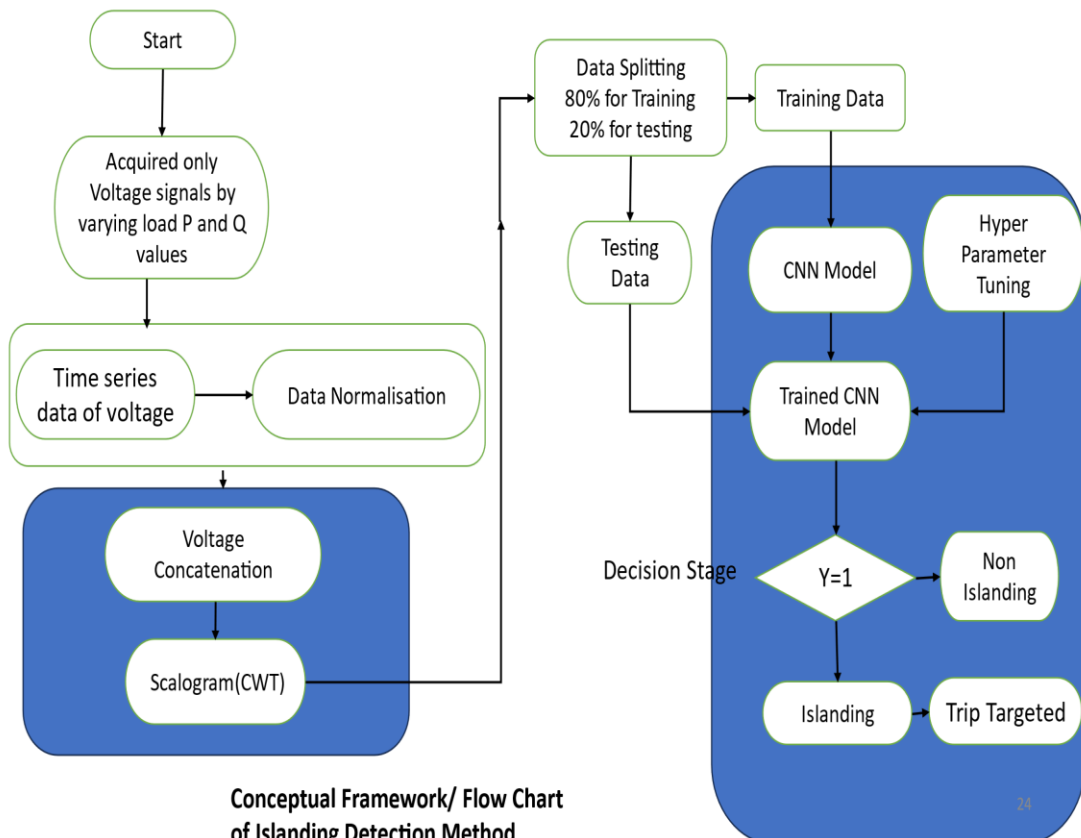
$$v_{t+1} = \rho v_t + \alpha \nabla J(W) \quad (10)$$

$$w_{t+1} = w_t - v_{t+1} \quad (11)$$

$$w_{new} = w_{old} - \alpha \nabla J(w_{old}) \quad (12)$$

ρ momentum

$\nabla J(W)$ gradient of the loss function



Conceptual Framework/ Flow Chart of Islanding Detection Method
FIGURE 5 Flow Chart of Islanding Detection Method

V. RESULTS AND DISCUSSION

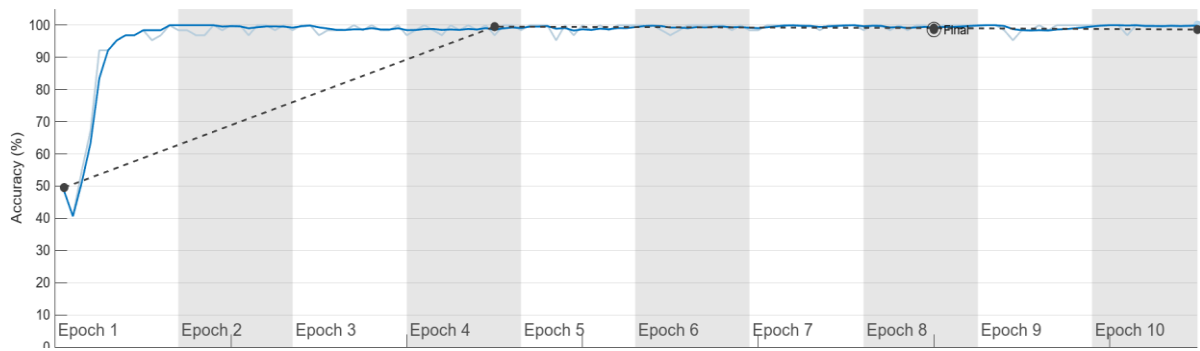


FIGURE 6 Accuracy vs Iterations

The above plot between Accuracy and Iterations, which is cluster of epochs, provides accuracy of the model with respect to iterations, started from 50% in its first epoch and reaches almost 90% in its first epoch and ends with 98.65% in its fourth epoch and maintained its accuracy till 130 iterations.

TABLE 2 Training and Validation Result

Validation Accuracy	98.65%
Epoch	10
Iterations	130
Iterations per Epoch	13
Maximum Iterations	130

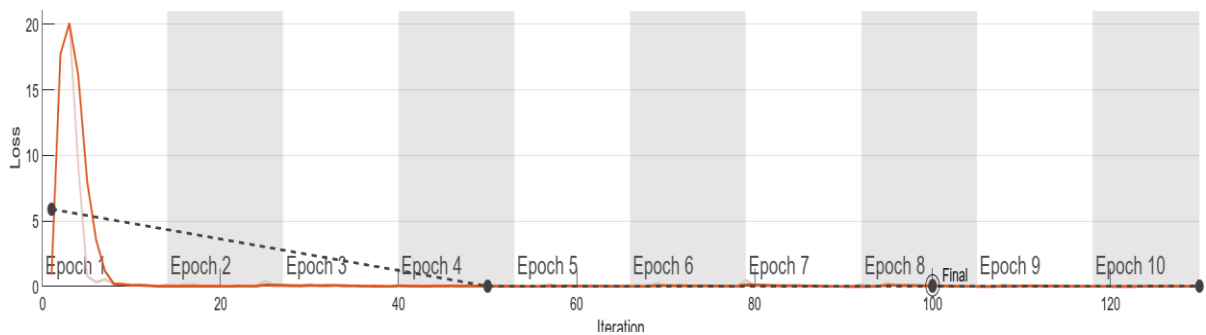
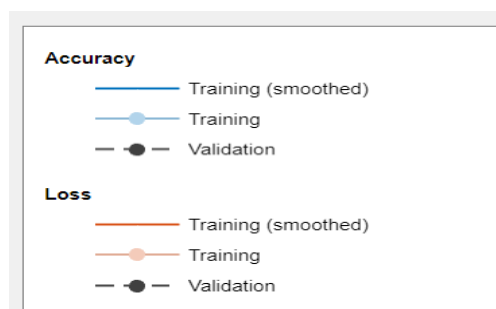


FIGURE 7 Loss Vs Iterations



From the above plot figure 5, it is observed that the value of loss is certainly decreased to almost less than one in its first epoch and maintained the same until 130iterations.

Further, the obtained result is experimented for hyperparameter tuning by using experiment manager, by initializing learning rate to 0.000001 under a trial, optimized further and reaches to the values provided in the table3.

TABLE 3Hyperparameter Tuning Results

Training Accuracy	98.43
Training loss	0.05
Validation Accuracy	99.09
Validation loss	0.04

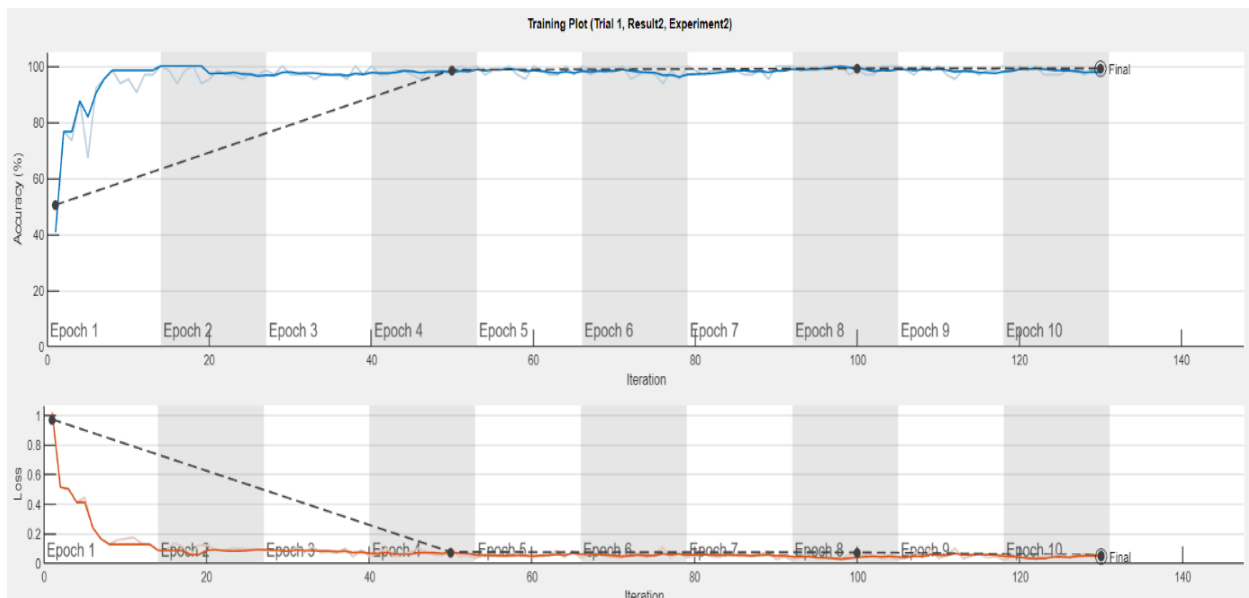
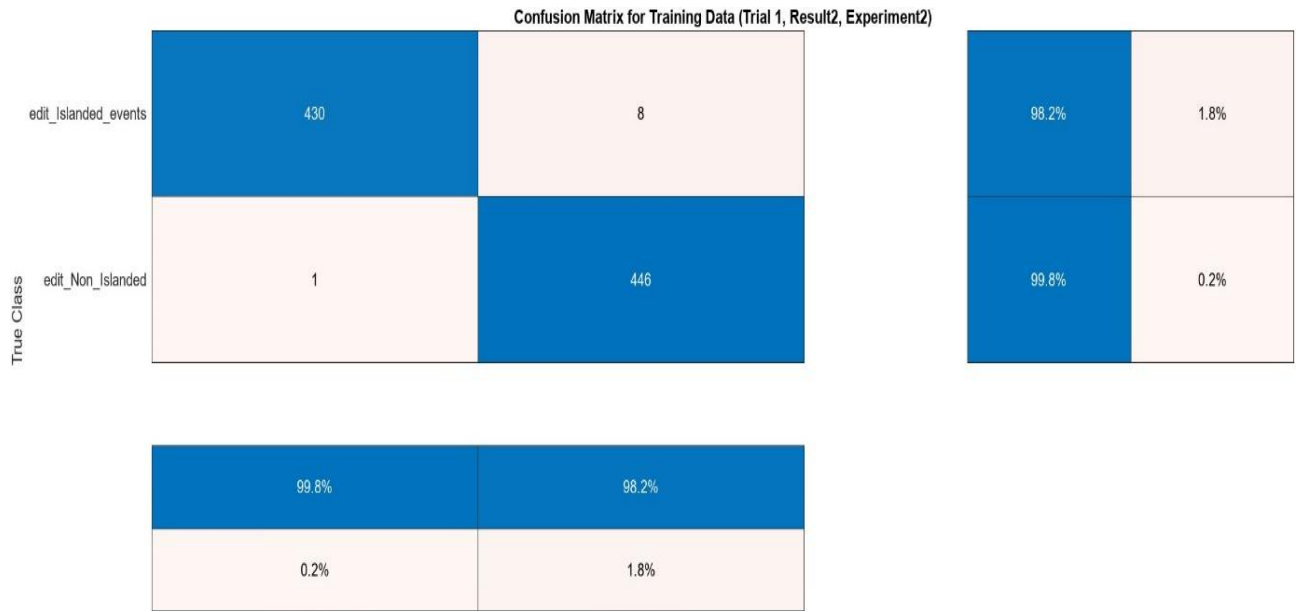
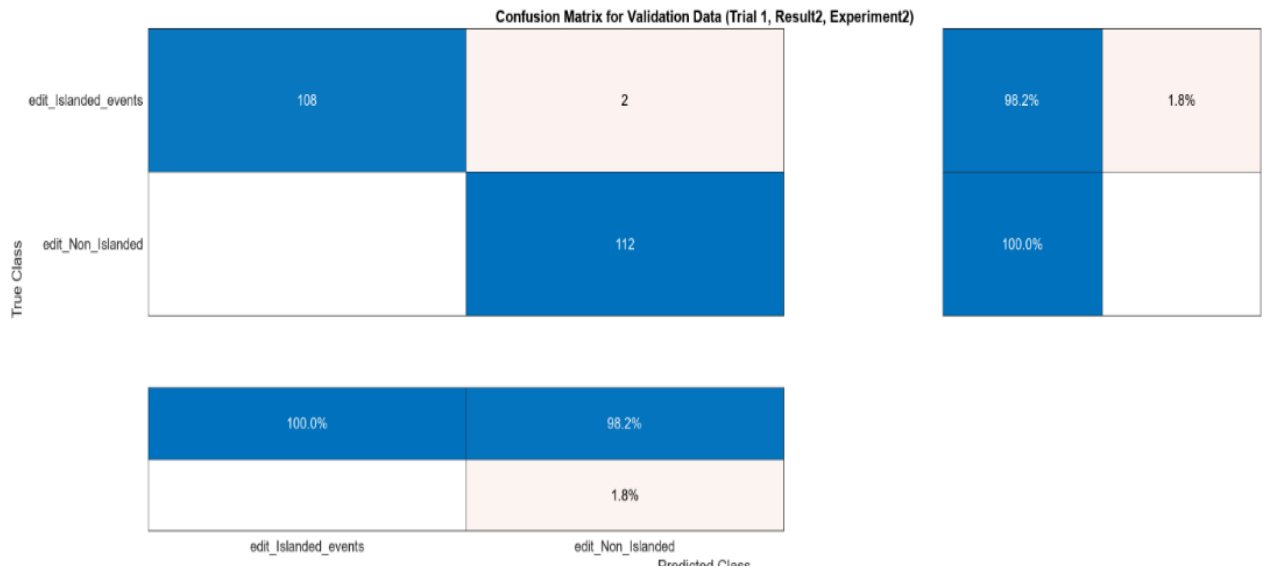


FIGURE 8Accuracy and loss Vs Iterations



MATRIX 1: Confusion Matrix for Training Data

From the above confusion matrix for training data, only 8 islanding observations were misclassified with 1.8% and 430 islanding events were classified with 99.2% accuracy against true class and 99.8% islanding events were classified against predicted class.



Matrix 2 Confusion Matrix for Validation Data

From the above matrix, it is evident that, 108 islanding events were classified against true class with 98.2% and 100% against predicted class and only 2 were misclassified with 1.8% against predicted class.

VI. CONCLUSION

In this paper, by using novel hybrid method, presented a classification of islanding and non-islanding occurrences for the proposed system, which consists PV module is integrated with utility with help of PCC. Scalogram is created with time series data recorded at PCC. A total 1107 observations have created under islanding and non-islanding in the presence of L-G fault with 0.2s and 100 samples per cycles of sampling frequency. The proposed IDT's performance of the model is obtained 98.65% validation accuracy and it is further experimented for hyper parameter tuning with different learning rates using experiment manager app,

training accuracy of 98.43% and 99.09% validation accuracy obtained shown in table and confusion matrix for training data and validation data. This shows that the proposed method is more accurate, which is very important for the emerging power system integrated with renewable sources.

References

- [1]. H. E. B. T. K. A Khamis, "A review of islanding detection techniques for renewable distributed generation systems," *Renew. Sustain Energy Rev*, vol. 28, pp. 483-493, 2013.
- [2]. A. H. C. H. K. a. A. Mehdi, "A comprehensive review of intelligent islanding schemes and feature selection techniques for distributed generation system," *IEEE Access*, vol. 9, no. 2021, pp. 146603-146624, 2021.
- [3]. C. L. C. C. Y. C. Y. K. L. Z. a. B. Fang, "A review of islanding detection method for microgrid," *Renew Sustain Energy Rev*, vol. 35, pp. 211-220, 2014.
- [4]. T. Basso, "IEEE 1547 and 2030 standards for distributed energy resources," *Nat. Renew. Energy Lab. (NREL), Golden, CO, USA, Tech. Rep*, 2014.
- [5]. T. T. F. M. M. R. B. S. G. a. J. G. R. M. Hudson, "Implementation and testing of anti-islanding algorithms for IEEE 929-2000 compliance of single phase photovoltaic inverters," *Proc 29th IEEE Photovolt. Spec. Conf. IEEE*, pp. 1414-1419, may 2002.
- [6]. C. H. K. T. G. S. B. A. B. M. S. u. Z. S. B. a. Y. S. O. R. Haider, "Passive islanding detection scheme based on autocorrelation function of modal current envelope for photovoltaic units," *IET Gener., Transmiss. Distrib.*, vol. 12, pp. 726-736, Feb 2018.
- [7]. E. F. E.-S. a. M. M. A. S. H. H. Zeineldin, "Impact of DG interface control on islanding detection and nondetection zones," *IEEE Trans. Power Del.*, vol. 12, no. no 3, pp. 1515-1523, July 2006.
- [8]. S. K. G. Manikonda and D. N. Gaonkar, "Comprehensive review of IDMs in DG systems," *IET Smart Grid*, vol. 2, no. no 1, pp. 11-24, 2019.
- [9]. M. J. S. D. a. M. A. S. M. S. D. Kermany, "Hybrid islanding detection in microgrid with multiple connection points to smart grids using fuzzy-neural network," *IEEE Trans. Power Syst.*, vol. 32, no. 4, pp. 2640-2651, July 2017.
- [10]. C.-H. K. Y.-S. O. G.-J. C. a. J.-S. S. J.-S. Kim, "An islanding detection method for multi-RES systems using the graph search method," *IEEE Trans. Sustain. Energy*, vol. 11, no. no 4, pp. 2722-2731, Oct 2020.
- [11]. S. B. A. B. R. H. T. G. a. C.-H. K. S. Admasie, "A passive islanding detection scheme using variational mode decomposition-based mode singular entropy for integrated microgrids," *Electr. Power Syst. Res*, vol. 177, no. Art No 105983, Dec .2019.
- [12]. H. H. Zeineldin and S. Kennedy, "Sandia frequency-shift parameter selection to eliminate nondetection zones," *IEEE Trans. Power Del.*, vol. 24, pp. 486-487, Jan 2009.
- [13]. R. K. M. a. S. D. P. Nayak, "Novel hybrid signal processing approach based on empirical mode decomposition and multiscale mathematical morphology for islanding detection in distributed generation system," *IET Gener., Transmiss. Distrib.*, vol. 14, no. no 26, pp. 6715-6725, Dec 2020.
- [14]. D. J. D. W. S. R. e. al, "ImageNet a large-scale hierarchical image database," *IEEE conf computer vision and Pattern Recognition*, no. 16 August 2018, 2009.
- [15]. L. C. C. B. C. Yann, "THE MNIST DATABASE of handwritten digits," no. 16 August 2018.